Journal of Power Sources 195 (2010) 6893–6896

Contents lists available at ScienceDirect

Journal of Power Sources

journal homepage: www.elsevier.com/locate/jpowsour

Short communication

Electrochemical lithium storage of TiO_2 hollow microspheres assembled by nanotubes

Jizhang Chen, Li Yang*, Yufeng Tang

School of Chemistry and Chemical Engineering, Shanghai Jiaotong University, No. 800 Dongchuan Road, MinHang District, Shanghai 200240, PR China

ARTICLE INFO

Article history:
Received 20 December 2009
Received in revised form 1 March 2010
Accepted 3 April 2010
Available online 10 April 2010

Keywords:
Hollow microsphere
Nanotube
Lithium-ion battery
TiO_2
Anatase

ABSTRACT

TiO_2 hollow microspheres with the shell consisting of nanotubes have been successfully synthesized via a template-free hydrothermal process and subsequent treatments. The electrochemical properties of the anatase sample have been investigated by cyclic voltammetry and galvanostatic method. The initial Li insertion/extraction capacity at a current density of 0.2 C reach 290 and 232 mAh g^{-1} respectively. Moreover, as-prepared TiO_2 delivers a reversible capacity of ca. 150 mAh g^{-1} after 500 cycles at 1 C, and it also shows superior high rate performance (e.g., 90 mAh g^{-1} at 8 C) without any modification.

© 2010 Elsevier B.V. All rights reserved.

1. Introduction

There have been considerable efforts directed to the fabrication of nanomaterials for lithium-ion batteries during the past few years [1–3]. Compared with micrometer-sized bulk materials, nanostructured electrodes exhibit better electrochemical performances, which are attributed to shortened diffusion length for ion transport, increased electrode–electrolyte contact area, reduced volumetric change, accommodation of the lattice stress, and a large excess surface and interface lithiation. Nevertheless, nanostructured electrodes also have some serious drawbacks, such as low thermodynamic stability and difficulty of handling. To solve these problems, developing nano-/micro-hierarchical electrode materials is a good choice [4]. Besides the advantages of nanometer-sized building blocks, nano-/micro-hierarchical electrode materials also possess the merits (e.g., thermodynamic stability) of micro- or submicrometer-sized assemblies. In this regards, they can guarantee less agglomeration and better strain relaxation upon cycling.

Being readily available, chemically stable, inexpensive, and environmentally benign, nanostructured TiO_2 has been recognized as an alternative anode material for lithium-ion batteries, due to its high rate performance, stable capacity retention, and safe operation [5–7]. TiO_2 hollow spheres have been prepared using multiple methods including templating method, hydrothermal process, spray pyrolysis, and sol–gel method [8–12]. In this communication, we developed a facile hydrothermal route and the subsequent treatments to prepare TiO_2 hollow microspheres with the shell assembled by nanotubes without templates or surfactants in the reaction system. To our knowledge, TiO_2 with such morphology has never been reported before. The as-prepared TiO_2 was evaluated as the electrode material, indicating it is an ideal host for rapid and efficient Li insertion/extraction.

2. Experimental

2.1. Synthesis and characterization of TiO_2 hollow microspheres

The precursor of our hydrothermal reaction was monodispersed amorphous spherical TiO_2 particles prepared by controlled hydrolysis of titanium tetraisopropoxide (TTIP, Ti-$(OC_3H_7)_4$, 97%, Aldrich) in ethanol + water solution reported in previous reference [13]. 4 mmol precursor and 1 mL 1% hydrogen peroxide were dispersed in 20 mL mixed solvent of 0.2 M NaOH aqueous solution and ethanol with the volume ratio being 1:1. After stirred for 10 min, the suspension was transferred into a 30 mL Teflon-lined stainless autoclave, which was maintained at 180 °C for 12 h and then cooled to room temperature naturally. The resulting white precipitate was recovered by centrifugation and immersed in 0.1 M HCl solution, and then washed with deionized water several times until the pH was 7, followed by calcination at 450 °C for 5 h in the air.

The structure and morphology of the products were characterized using X-ray diffraction measurement (XRD, Rigaku, D/max-Rbusing Cu Ka radiation), transmission electron microscopy (TEM, JEOL JEM-2010 equipped with Energy Dispersive X-ray

* Corresponding author. Tel.: +86 21 54748917; fax: +86 21 54741297.
E-mail address: liyangce@sjtu.edu.cn (L. Yang).

0378-7753/$ – see front matter © 2010 Elsevier B.V. All rights reserved.
doi:10.1016/j.jpowsour.2010.04.005

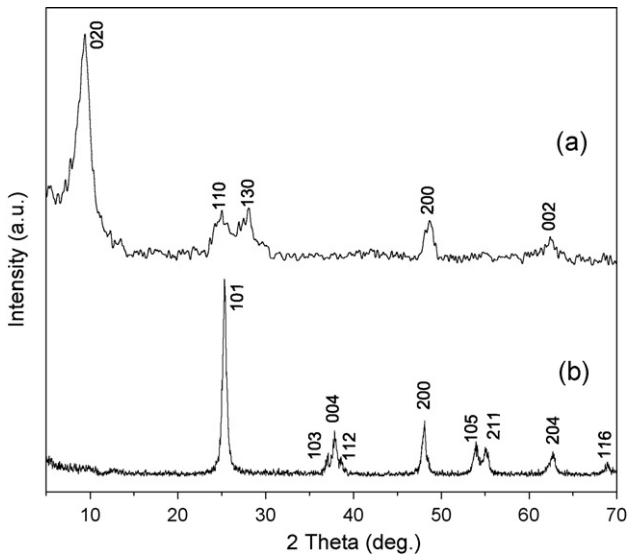

Fig. 1. XRD patterns of the products (a) before and (b) after calcination.

Detector) and field emitting scanning electron microscopy (FE-SEM, JEOL JSM-7401F) respectively.

2.2. Electrode preparation and electrochemical characterization

The electrochemical behavior was measured with coin cells in which a lithium metal foil was used as the counter electrode. The electrolyte employed was 1 M solution of $LiPF_6$ in ethylene carbonate and dimethyl carbonate (EC + DMC) (1:1 in volume). The composite electrodes were made of the active materials powder (80 wt%), acetylene black (10 wt%) and polyvinylidene fluoride (PVDF) binder (10 wt%) homogeneously mixed in N-methyl pyrrolidinone (NMP) solvent and then coated uniformly on an aluminium foil. Finally, the electrode was dried under vacuum at 110 °C for 10 h. Cell assembly was carried out in an argon-filled glove box (German, M. Braun Co., $[O_2] < 1$ ppm, $[H_2O] < 1$ ppm). The coin cells were cycled under different current densities between cutoff voltages of 3.0 and 1.0 V on a CT2001A cell test instrument (LAND Electronic Co.) at room temperature. A CHI604b Electrochemical Workstation was used for cyclic voltammetry measurements.

3. Results and discussion

XRD patterns of the as-prepared samples before and after calcination are depicted in Fig. 1. The observed broad peaks in Fig. 1a are

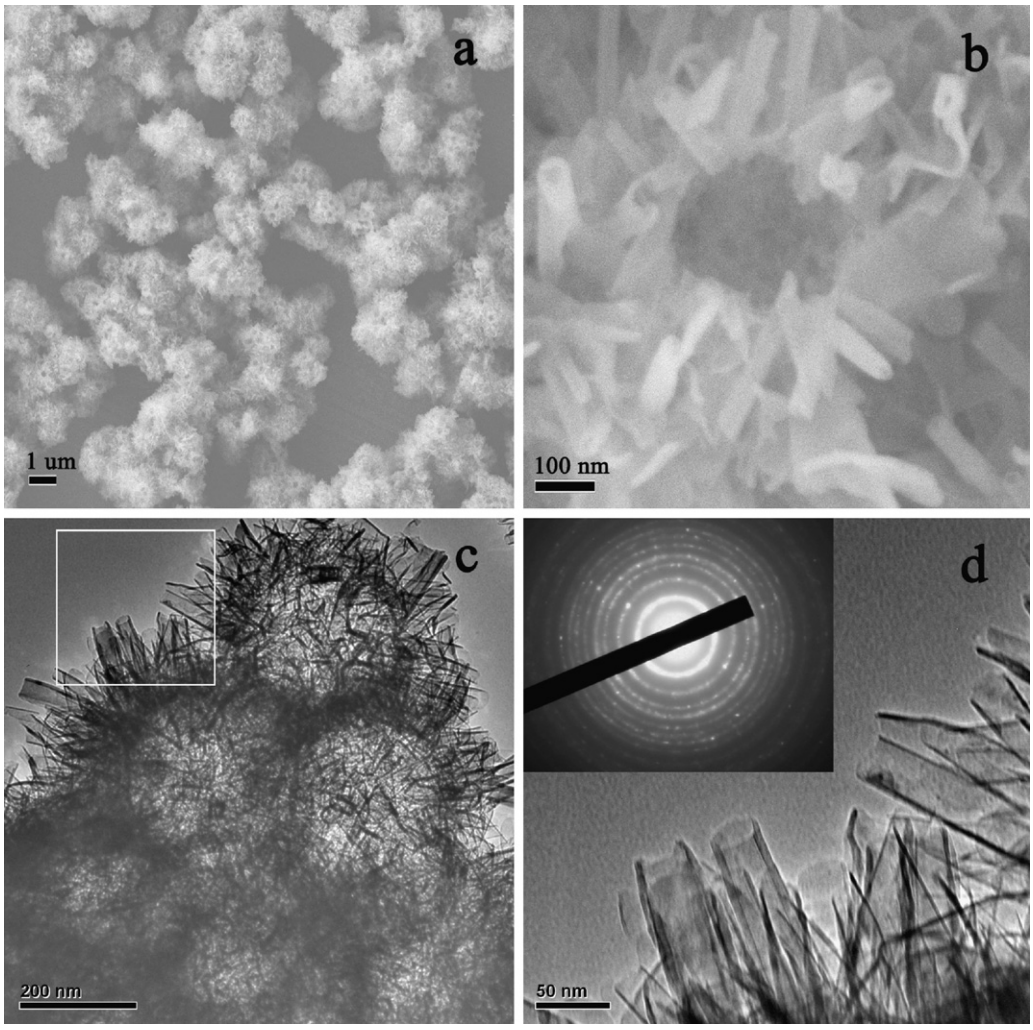

Fig. 2. (a, b) SEM and (c, d) TEM images of the as-prepared products at different magnifications. (Inset: SAED pattern taken from a nanotube.)

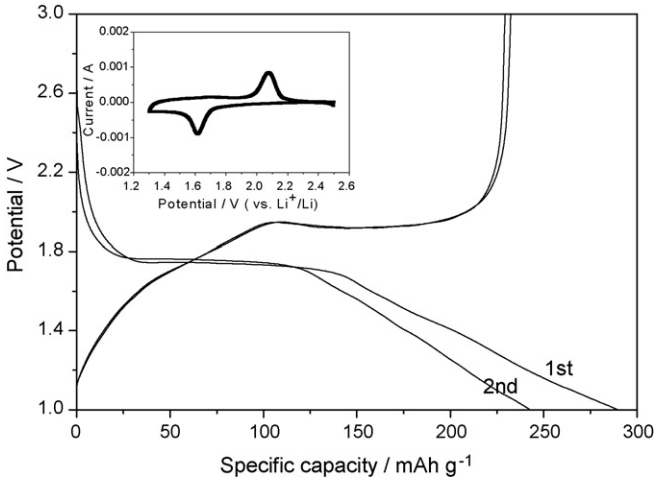

Fig. 3. Initial two discharge/charge curves of as-prepared TiO_2 electrodes at 0.2 C and cyclic voltammogram (inset) at a scan rate of 0.2 mV s^{-1}.

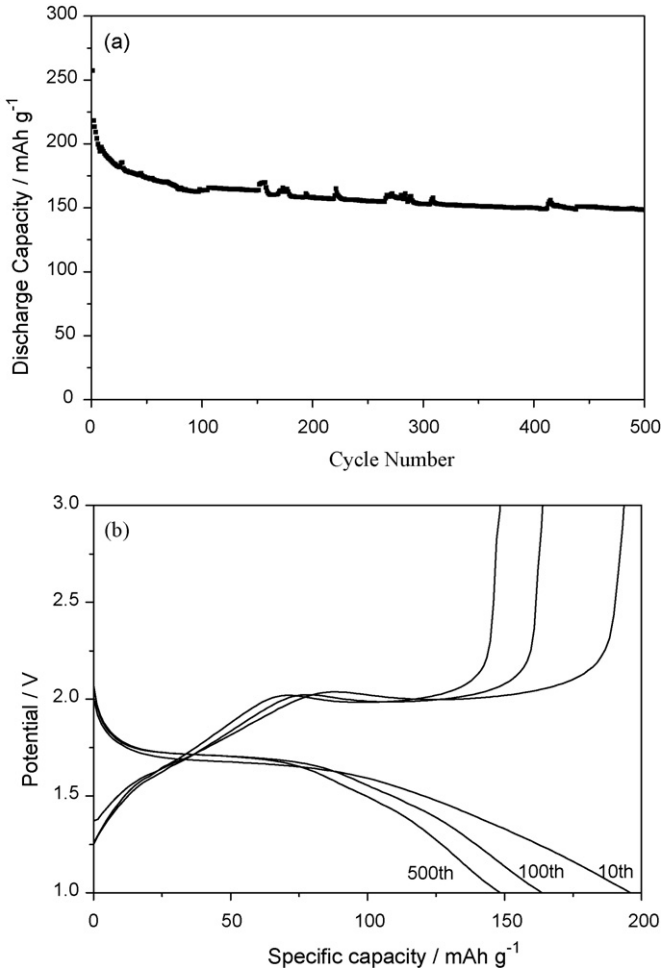

Fig. 4. (a) Discharge capacity of as-prepared TiO_2 electrodes depending on the number cycles for 500 cycles at 1 C and (b) galvanostatic curves of 10th, 100th, 500th cycles.

in good agreement with orthorhombic $H_xTi_{2-x/4}\Upsilon_{x/4}O_4{\cdot}H_2O$ [14]. As shown in Fig. 1b, sharp peaks appear after calcination, and they are well matched to the diffraction peaks of anatase TiO_2 (JCPDS 65-5714), without any other phases such as rutile, brookite, TiO_2(B), and residual protonated titanate, demonstrating the temperature and time used in calcination were enough to convert protonated titanate to pure anatase TiO_2. Furthermore, the sharpening of Bragg peaks suggests the obtained TiO_2 is well crystallized, accompanied by the increase of crystallite size over calcination. The average crystalline size of as-prepared TiO_2, determined from diffraction peaks using the Scherrer's formula, is ca. 18 nm.

The morphology and structure of the products were assessed using FE-SEM and TEM measurements. Fig. 2a shows a panoramic SEM image of as-prepared TiO_2, which is composed of uniform spheres with a rough surface. A single broken sphere with the shell assembled by open-ended nanotubes of ca. 200 nm in length is clearly observed in Fig. 2b, indicating its hollow structure. Fig. 2c shows several microspheres with the diameter of ca. 400 nm. The unambiguous contrast between the dark edge and the gray center of each microsphere further confirms the hollow structure. A magnified area from Fig. 2c is presented in Fig. 2d, clearly demonstrating that the nanotubes are ca. 30 nm in diameter and 5 nm in wall thickness, respectively. SAED rings (inset of Fig. 2d) reveal that the nanotubes consist of polycrystalline anatase TiO_2 and the all the rings can be indexed as anatase phase which is consistent with the preceding XRD result.

Fig. 3 displays the initial two discharge/charge curves of the TiO_2 electrodes with cutoff voltages of 3.0–1.0 V (versus Li^+/Li) at 0.2 C (67.4 mA g^{-1}) and the cyclic voltammogram (inset) at a scan rate of 0.2 mV s^{-1}. There are distinct potential plateaus at ca. 1.78 and 1.98 V in the discharge/charge curves, corresponding to Li^+ insertion into and extraction from anatase lattice [15,16]. The discharge curve can be divided into three domains. The first domain is the monotonous potential decrease, induced by a solid solution insertion mechanism linked to small particle and crystalline sizes [17]. The second domain with the constant potential at ca. 1.78 V relates to Li^+ insertion into and extraction from the interstitial octahedral site of TiO_2 reversibly, during which a two-phase reaction occurs with phase equilibrium of the Li-poor $Li_{0.01}TiO_2$ (tetragonal) phase and the Li-rich $Li_{0.55}TiO_2$ (orthorhombic) phase [18,19]. The third domain is a sloped potential, associated with lithium storage in the surface as well as the formation of Li_1TiO_2 phase [20]. The initial discharge and charge capacity are 290 and 232 mAh g^{-1} with corresponding insertion coefficient of 0.86 and 0.69, respectively. It can be clearly seen that the initial charge curve is the reverse process of the discharge curve and the reversible efficiency is as high as 80%. In the second cycle, the insertion and extraction capacities are observed to be 242.7 and 229.3 mAh g^{-1}. The irreversible capacity of 13.4 mAh g^{-1} is much smaller than that (ca. 58 mAh g^{-1}) of the initial cycle.

CV measurement using a san rate of 0.2 mV s^{-1} with cutoff voltages of 2.5–1.3 V (versus Li^+/Li) is shown as an inset of Fig. 3. One pair of apparent cathodic/anodic peaks located at 1.6 and 2.1 V (versus Li^+/Li) can be observed, which is in accordance with the plateaus of the discharging/charging curves though there is a little deviate originating from the high scan rate. The ratio of anodic to cathodic peak currents is nearly 1 and the voltammetric area of the discharging/charging branches is almost equal, demonstrating the lithium storage is highly reversible and this redox system remains in equilibrium throughout the potential scan.

Fig. 4a presents the cycling performance of TiO_2 hollow microspheres at a current density of 1 C. They suffer from significant capacity fading in the initial 80 cycles, and then deliver favorable cycle stability. Up to 150 mAh g^{-1} is obtained after 500 cycles and the average capacity loss from the 2nd to 500th cycles is ca. 0.14 mAh g^{-1} per cycle, manifesting exceptional capacity retention. The serious capacity loss in the initial cycles (especially initial six) can be attributed to the adsorbed trace water and irreversible Li insertion sites (i.e., surface defects such as surface vacancies or voids connected to structural distortion caused by Jahn–Teller effect), respectively [21]. The trace water and irreversible sites are

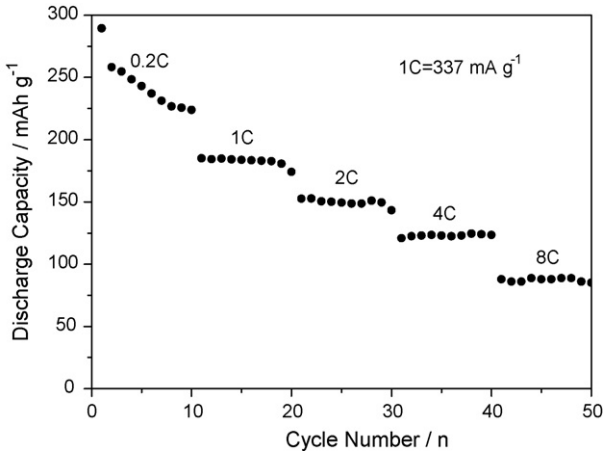

Fig. 5. Discharge capacity of as-prepared TiO_2 electrodes from 0.2 C to 8 C for 10 cycles at each rate.

consumed gradually and the residual lithium in the electrode could improve electric conductivity, thus leading to good capacity maintenance in the subsequent cycles. Galvanostatic curves of 10th, 100th, and 500th cycles are given in Fig. 4b. 10th cycle shows a little difference (ca. 1.6 mAh g^{-1}) of discharge and charge capacities, while 100th and 500th cycles both exhibit almost the same discharge and charge capacities, demonstrating excellent reversibility.

The rate capacity behavior of the TiO_2 hollow microspheres at different current densities is illustrated in Fig. 5. A specific discharge capacity of 222 mAh g^{-1} is obtained at 0.2 C, and then drops to 185, 150, 125, 90 mAh g^{-1} at 1, 2, 4, 8 C, respectively, exhibiting a favorable high rate performance which is comparable to mesoporous anatase TiO_2 without the doping of RuO_2 [22]. In short, the superior electrochemical lithium storage in TiO_2 hollow microspheres is derived from the intriguing hierarchical hollow micro-/nanostructured morphology, not only reducing ionic and electronic diffusion distance, but also providing a thermodynamically stable system, in which active materials contact sufficiently with the acetylene black and the electrolyte, and less agglomeration and better strain relaxation upon cycling are guaranteed.

4. Conclusion

In this article, anatase TiO_2 hollow microspheres with the diameter of ca. 400 nm and the shell assembled by nanotubes were synthesized successfully and investigated as the anode material in lithium-ion batteries. As-prepared TiO_2 with the unique morphology and intriguing physicochemical properties delivers a discharging capacity as high as 150 mAh g^{-1} after 500 cycles at 1 C, demonstrating satisfactory reversibility and cyclicity. Other measurements also show this material has a bright prospect when applied in lithium-ion batteries.

Acknowledgments

This work was supported by the National Key Project of China for Basic Research (Grant No. 2006CB202600) and the National High Technology Research and Development Program of China (Grant No. 2007AA03Z222). We thank the Instrumental Analysis Center of Shanghai Jiaotong University for Materials Characterization.

References

[1] P. Poizot, S. Laruelle, S. Grugeon, L. Dupont, J.M. Tarascon, Nature 407 (2000) 496.
[2] T. Zhang, L.J. Fu, J. Gao, Y.P. Wu, R. Holze, H.Q. Wu, J. Power Sources 174 (2007) 770.
[3] S.M. Paek, E.J. Yoo, I. Honma, Nano Lett. 9 (2009) 72.
[4] Y.G. Guo, J.S. Hu, L.J. Wan, Adv. Mater. 9999 (2008) 1.
[5] S.W. Kim, T.H. Han, J. Kim, H. Gwon, H.S. Moon, S.W. Kang, S.O. Kim, K. Kang, ACS Nano 3 (2009) 1085.
[6] H.G. Jung, S.W. Oh, J. Ce, N. Jayaprakash, Y.K. Sun, Electrochem. Commun. 11 (2009) 756.
[7] H. Qiao, Y.W. Wang, L.F. Xiao, L.Z. Zhang, Electrochem. Commun. 10 (2008) 1280.
[8] W.H. Shen, Y.F. Zhu, X.P. Dong, J.L. Gu, J.L. Shi, Chem. Lett. 34 (2005) 840.
[9] C.Y. Song, W.J. Yu, B. Zhao, H.L. Zhang, C.J. Tang, K.Q. Sun, X.C. Wu, L. Dong, Y. Chen, Catal. Commun. 10 (2009) 650.
[10] J.K. Zhou, L. Lv, J.Q. Yu, H.L. Li, P.Z. Guo, H. Sun, X.S. Zhao, J. Phys. Chem. C 112 (2008) 5316.
[11] S. Nagamine, A. Sugioka, H. Iwamoto, Y. Konishi, Powder Technol. 186 (2008) 168.
[12] Y.X. Zhang, G.H. Li, Y.C. Wu, T. Xie, Mater. Res. Bull. 40 (2005) 1993.
[13] Y.W. Wang, H. Xu, X.B. Wang, X. Zhang, H.M. Jia, L.Z. Zhang, J.R. Qiu, J. Phys. Chem. B 110 (2006) 13835.
[14] T. Sasaki, M. Watanabe, H. Hashizume, H. Yamada, H. Nakazawa, J. Am. Chem. Soc. 118 (1996) 8329.
[15] Y.F. Wang, M.Y. Wu, W.F. Zhang, Electrochim. Acta 53 (2008) 7863.
[16] J. Li, Y.L. Jin, G.X. Zhang, H. Yang, Solid State Ionics 178 (2007) 1590.
[17] G. Sudant, E. Baudrin, D. Larcher, J.M. Tarascon, J. Mater. Chem. 15 (2005) 1263.
[18] M. Wagemaker, A.A. Van Well, G.J. Kearley, F.M. Mulder, Solid State Ionics 175 (2004) 191.
[19] M.V. Koudriachova, S.W. De Leeuw, Phys. Rev. B 69 (2004) 054106.
[20] M. Wagemaker, W.J.H. Borghols, F.M. Mulder, J. Am. Chem. Soc. 129 (2007) 4323.
[21] G.F. Ortiz, I. Hanzu, P. Knauth, P. Lavela, J.L. Tirado, T. Djenizian, Electrochim. Acta 54 (2009) 4262.
[22] Y.G. Guo, Y.S. Hu, W. Sigle, J. Maier, Adv. Mater. 19 (2007) 2087.